Sum-frequency mixing of radiation from two extended-cavity laser diodes using a doubly resonant external cavity for laser cooling of trapped ytterbium ions

Kazuhiko Sugiyama,[1,2,*] Sho Kawajiri,[1] Nobuhiko Yabu,[1]
Kanehiro Matsumoto,[1] and Masao Kitano[1,2]

[1]Graduate School of Electronic Science and Engineering, Kyoto University, Katsura, Nishikyo, Kyoto 615-8510, Japan

[2]PRESTO/CREST, Japan Science and Technology Corporation, 4-1-8 Honcho Kawaguchi, Saitama 332-0012, Japan

*Corresponding author: sugiyama@kuee.kyoto-u.ac.jp

Received 28 June 2010; accepted 24 August 2010;
posted 1 September 2010 (Doc. ID 130699); published 5 October 2010

Over 100 μW of continuous-wave tunable ultraviolet radiation at 370 nm is generated by the sum-frequency mixing of radiation from two extended-cavity laser diodes having powers of 60 mW at 822 nm and 8 mW at 671 nm in a lithium iodate crystal. The crystal is placed in an external cavity that enhances the powers of two fundamental beams simultaneously by approximately 40. This light source is successfully applied to the laser cooling of trapped ytterbium ions.

OCIS codes: 190.2620, 300.6520, 020.3320, 140.2020.

1. Introduction

Single-frequency continuous-wave ultraviolet (UV) radiation is required for high-resolution spectroscopy and for the laser cooling of atoms and ions. Light sources based on laser diodes (LDs) are found to be quite useful because they are compact, inexpensive, consume less power, and have a long lifetime. These characteristics are desirable for applications such as optical frequency standards, where continuous operation is essential.

The singly ionized ytterbium ion (Yb^+) is one of the attractive ion species that provide reference or clock transitions that are used in optical frequency standards [1,2] and that are used for quantum information processing [3]. In these applications, ions are trapped and their translational energies are reduced by laser cooling in order to confine them in the Lamb–Dicke region. For Yb^+, the $^2S_{1/2} - {}^2P_{1/2}$ transition at 370 nm is driven for laser cooling. As a 370 nm light source based on LDs for the laser cooling of Yb^+, the second-harmonic generation (SHG) of LD radiation at 740 nm is developed [3,4]. In the UV region, LDs having a wavelength as low as 370 nm have recently been developed, and the laser cooling of Yb^+ is realized by an extended-cavity laser diode (ECLD) [5] using a UV-LD chip [6].

As an alternative approach, we develop a 370 nm light source by sum-frequency mixing (SFM) of radiation from two LDs having wavelengths of 822 and 671 nm. For the LD having a wavelength of 822 nm, one can use a high-power single-transverse-mode LD chip in the 830 nm region in the extended-cavity configuration in order to increase the sum-frequency power. In addition, the wavelength of 822 nm is approximately twice as long as that of the $^2S_{1/2} - {}^2D_{5/2}$ clock transition in Yb^+, 411 nm, or the 6S-8S two-photon transition in the cesium atom [7]. This is convenient for the frequency stabilization of the sum frequency. For the LD having a wavelength of 671 nm, an antireflection (AR) coating of very low residual reflectivity on the output facet is required. This is because a linewidth of the order of several megahertz is still observed with many models of LD chips in the red region, even when one uses them in the extended-cavity configuration if they have no

0003-6935/10/295510-07$15.00/0

special AR coating. The linewidth of the light source is required to be much narrower than the natural width of the cooling transition in order to approach the Doppler-cooling limit. The $^2S_{1/2} - {}^2P_{1/2}$ cooling transition in Yb^+ has a natural linewidth of 20 MHz [8]. The linewidth of the ECLD using such a special AR-coated LD chip is expected to be narrower than 1 MHz even in the red region, and AR-coated LD chips in the 670 nm region are commercially available.

The power required for the laser cooling of trapped ions using strong transitions is estimated to be of the order of a few microwatts, because the ions are confined in a small space and the saturation intensity of the cooling transition is attained when a cooling beam of the order of a few microwatts is focused. Practically, a power of more than several tens of microwatts appears to be desirable. This allows one to use a cooling beam having a larger beam waist in the trap region in order to enlarge the cross section with uncooled ions at the beginning of cooling and to enable robustness against the misalignment of the beam to the ions.

In this work, we generate radiation having a power of more than 100 μW at 370 nm by the SFM of two ECLDs, and successfully apply it to the laser cooling of trapped Yb^+ ions. In order to increase the sum-frequency power, we place a nonlinear crystal for SFM in an external cavity. The cavity resonates at the frequencies of the two ECLDs. SFM using a doubly resonant external cavity was demonstrated in a system of separate external cavities for two fundamental beams, where the second harmonic of argon-ion laser radiation and radiation from a tapered-amplifier LD were mixed [9]. SFM using a doubly resonant single cavity for two fundamental beams, as in the case of our scheme, was carried out using the second harmonic of titanium-sapphire laser radiation and radiation from a tapered-amplifier LD [10]. To the best of our knowledge, our system represents the first application of SFM of radiation from two LDs using a doubly resonant external cavity.

When we first demonstrated this SFM scheme, we realized the storage of only a few Yb^+ ions in a radio-frequency (RF) trap, where the ions had been cooled using another light source having higher power. We could not cool and trap uncooled ions using only the sum-frequency radiation, because the sum-frequency power was approximately 10 μW owing to the rapid decrease in power caused by the damage induced by the generated UV light [11]. In this work, the generated sum-frequency exhibits a much slower decrease in power, and it is used for a light source for laser cooling without the use of other 370 nm light sources.

Section 2 describes our SFM system. In Section 3, we describe the performance of our SFM and present an analysis of the conversion efficiency. The results of the laser cooling of trapped Yb^+ by using this light source are also presented. In Section 4, we conclude this work.

2. Experimental Setup

Figure 1 shows a schematic of the SFM of radiation from two ECLDs. The system comprises two ECLDs and an external cavity that resonates at the wavelengths of the two ECLDs. Other optics for coupling the beams from the two ECLDs to the cavity and a system for locking the frequencies of the ECLDs to the cavity resonances are included.

A. Extended-Cavity Laser Diodes

The two LDs are used as ECLDs, where diffraction gratings are placed in the Littrow configuration to enable wavelength selectivity. The wavelengths of the ECLDs are 822 and 671 nm. The ECLD having a wavelength of 822 nm comprises a commercially available single-transverse-mode LD having an output power of 150 mW (Sanyo DL8032), a collimation lens having a numerical aperture (NA) of 0.55, and a diffraction grating having a pitch of 1800/mm and a

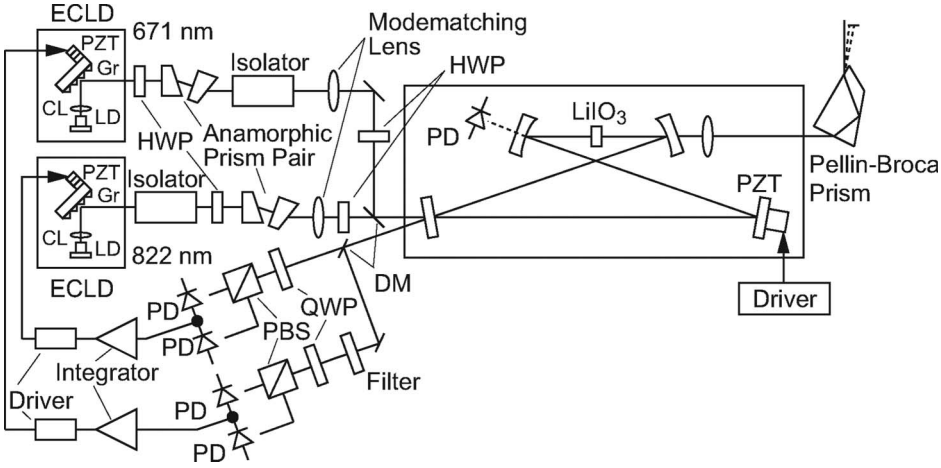

Fig. 1. Schematic of experimental setup for SFM of two extended-cavity laser diodes (ECLDs) using a doubly resonant external cavity: Gr, diffraction grating; CL, collimation lens; HWP, half-wave plate; QWP, quarter-wave plate; DM, dichroic mirror; PBS, polarization beam splitter; PD, photodiode.

blaze wavelength of 400 nm. The first-order diffraction, which is optically fed back to the LD chip, is measured to be 8% of the incident power from the LD chip, whereas 80% is reflected as the zeroth order and is used as an output of the ECLD. The small feedback ratio is sufficient to realize stable single-frequency oscillation in the ECLD. The distance between the LD chip and the diffraction grating is approximately 8 cm.

We tested the wavelength tuning range with a similar setup, including another LD chip from the same lot as that used in the SFM. The tuning range was between 815.0 and 836.7 nm, and the oscillation wavelength of the LD chip itself was 828.5 nm. The output power of the zeroth order reflection was between 103 and 113 mW; thus, a small decrease was observed as the wavelength approached the tuning limit. We measured the continuous frequency tuning range and the linewidth of the ECLD used in the SFM to be 4.4 GHz and narrower than 500 kHz, respectively. The linewidth is determined from the beat note with another ECLD having a linewidth narrower than 50 kHz, which is fast-fed back to the resonance of a confocal cavity.

For the ECLD having a wavelength of 671 nm, we use a commercially available AR-coated LD chip (Sacher SAL675-10). One can expect a linewidth narrower than 1 MHz in the ECLD using an AR-coated LD chip; however, because we have only one AR-coated chip at this wavelength, we were unable to evaluate the linewidth by beat measurement. The NA of the collimation lens is 0.55. The pitch and blaze wavelength of the diffraction grating are 1800/mm and 200 nm, respectively. The first-order diffraction, which is optically fed back to the LD chip, is measured to be 5% of the incident power from the LD chip, whereas 86% is reflected as the zeroth order and is used as an output of the ECLD. The distance between the LD chip and the diffraction grating is approximately 10 cm.

The wavelength tuning is as follows. The shortest wavelength is 664 nm with an output power of 4.5 mW, the wavelength is 673 nm with a peak output power of 14.5 mW, and the longest wavelength is 678 nm with an output power of 6 mW. An output power of 13.5 mW is obtained at 671 nm. The continuous tuning range is 3.3 GHz.

The output beam of each ECLD is circularized to the minor axis of the output beam using an anamorphic prism pair. The polarization of each beam is adjusted by a zeroth order quartz half-wave plate as the beam passes through the angled faces of the anamorphic prisms, approximately at the Brewster angle. Each beam also passes through an optical isolator having an isolation of 60 dB in order to minimize the optical feedback to the ECLD. To avoid damage to the polarizers in the optical isolator, the isolator is placed before beam circularization for the beam from the ECLD having a wavelength of 822 nm.

B. External Cavity

The external cavity comprises four mirrors in a bow-tie configuration, as shown in Fig. 1. Two concave mirrors having a curvature of 50 mm are used to focus the two beams at the center of the nonlinear crystal for SFM. The free spectral range of the cavity is 770 MHz, i.e., the cavity length is 390 mm. The coatings of all the mirrors except the input coupler are the same: The reflectivities at 822 and 671 nm are greater than 0.999, and the transmissivity at 370 nm is 0.925 ± 0.025. The reflectivities of the input coupler are 0.97 ± 0.003 at 671 and 822 nm. A high-reflection flat mirror is mounted on a piezoelectric transducer (PZT) fixed on a mirror mount. The cavity length is controlled by the voltage applied to the PZT. The intracavity powers of the two fundamental beams are monitored by detecting the beams leaking through the concave mirror before the crystal using a photodiode. The cavity is placed in an aluminum box having two AR-coated glass windows.

A 3 mm long lithium iodate ($LiIO_3$) crystal is used as a nonlinear crystal for SFM. The crystal is cut to $\theta = 47.9°$ to achieve Type I phase matching approximately to the normal incidence of the two fundamental beams at 822 and 671 nm. The two crystal facets have single-layer coatings in order to decrease the reflectivities at 822 and 671 nm. The reflectivities at each facet are 0.005, 0.003, and 0.09 at 822, 671, and 370 nm, respectively, according to the data measured by the manufacturer.

The two beams from the ECLDs are collinearly combined using a dichroic mirror before entering the external cavity. The two beams from the ECLDs are focused using separate lenses to realize independent mode matching. Before the dichroic mirror, two mirrors fixed on adjustable mounts are used to independently align each beam to the cavity (not shown in the figure). The polarizations of the two beams are adjusted to be the same and *s* polarization to the cavity mirrors in order to realize Type I phase matching and higher reflectivities, respectively. The sum-frequency beam transmitted through the concave mirror after the crystal is collimated using a lens and then separated from the two fundamental beams using a Pellin–Broca prism.

The frequencies of the two ECLDs are locked to the cavity resonances by using a polarization spectroscopic technique [12]. The two fundamental beams reflected from the external cavity are separated using a dichroic mirror. The polarization spectroscopic signal of each beam is detected using a system comprising a quarter-wave plate, a polarization beam splitter, and a differential photodiode. A small reflection at 822 nm at the dichroic mirror changes the zero-crossing point of the error signal of the 671 nm beam because the power of the ECLD at 671 nm is 1 order of magnitude smaller than that at 822 nm. Therefore, a filter for the rejection of the residual power at 822 nm is inserted into the beam pass at 671 nm. After the frequencies of the two ECLDs are locked to the cavity resonances,

the sum frequency is swept by changing the voltage applied to the PZT to control the cavity length.

3. Results and Analysis

A. Performance of Sum-Frequency Mixing

Figures 2(a) and 2(b) show the resonance signals and the polarization spectroscopic signals of the cavity by the two ECLDs, respectively, obtained by linearly sweeping the voltage applied to the PZT to control the cavity length. From the resonance signals, we estimated the finesses of the cavity to be 110 and 120 at 671 and 822 nm, respectively. The stretch of the PZT with the applied voltage exhibits a nonlinearity, and we measured the deviation from the linear sweep to be 30%. However, we used the values of the finesse determined by the voltage sweep of the PZT to evaluate the sum-frequency power relative to the theoretically estimated value. Figure 2(c) shows the resonance signals and the polarization spectroscopic signals when the servo loops were closed. The servo bandwidth was 2 kHz for each ECLD.

Figure 3 shows the dependence of sum-frequency power on the two fundamental powers. The sum-frequency power and the two fundamental powers were measured after the prism and at the input window of the box, respectively. The sum-frequency power linearly increased with each fundamental power within the power range in this work. The maximum sum-frequency power of 116 μW was generated from the fundamental power of 8.3 and 62 mW at 671 and 822 nm, respectively.

We theoretically estimate the sum-frequency power. In the following equations, the subscripts 1, 2, and 3 refer to the 822, 671, and 370 nm beams, respectively. The sum-frequency power using a doubly resonant external cavity is given by

$$P_3 = (\gamma_{M1} A_1 P_1)(\gamma_{M2} A_2 P_2)\gamma_S, \tag{1}$$

where γ_{Mi}, A_i, and P_i are the mode-matching efficiencies to the external cavity, the fundamental enhancement factors by using the external cavity, and the powers of the beams, respectively. γ_S is the single-pass conversion efficiency at phase matching, and it is given by

$$\gamma_S = (4\omega_1\omega_2\omega_3/\pi\epsilon_0 c^4 n_3^2) d_{\text{eff}}^2 l h(B, \xi_i), \tag{2}$$

from the theory of Boyd and Kleinman for the case in which the absorption of each beam in the crystal is negligibly small [13], where d_{eff} is the effective nonlinear coefficient, ϵ_0 is the electric constant, c is the speed of light, ω_i are the angular frequencies of the beams, n_i are the refractive indices, l is the crystal length, and $h(B, \xi_i)$ is a dimensionless focusing function introduced by Boyd and Kleinman [13], where B is the double-refraction parameter defined as $B = \rho[l(k_1 + k_2)/2]^{1/2}/2$ in the case of SFM [14], ρ is the walk-off angle, and k_i are the propagation constants in the crystal. ξ_i are the focusing parameters defined as $\xi_i = l/b_i$, where $b_i = w_{0i}^2 k$ are the confocal parameters and w_{0i} are the radii of the fundamental beams at the focus.

From the known Sellmeier equation [15], we calculate n_3, ρ, and the angle of phase matching to be 1.872, 0.090 rad (or 5.2°), and 47.2°, respectively. From the equation $d_{\text{eff}} = d_{31}\sin(\theta + \rho)$ [16], we obtain $d_{\text{eff}} = 4.0$ pm/V, using the nonlinear coefficient $d_{31} = 4.4$ pm/V, measured with the SHG of radiation at 1064 nm [17] and correcting it for the dispersion in the nonlinear coefficient [16–18] to increase d_{31} by 14%. The value of B is calculated to be 10. In the design of the cavity, ω_{01} and ω_{02} in the nonlinear crystal are 24 and 20 μm, respectively. The corresponding focusing parameters ξ_1 and ξ_2 are 0.36 and 0.40, respectively. From the values of B and ξ_i, we estimate that the value of h is approximately 0.05, then we obtain the value of γ_S to be $3.9 \times 10^{-4}\text{W}^{-1}$. The mode matching efficiencies γ_{M1} and γ_{M2} are estimated to be 0.91 and 0.76 from the ratio between the transmission power in the TEM_{00} mode and the sum of those in other modes for each beam, determined from Fig. 2(a). We determine the fundamental enhance-

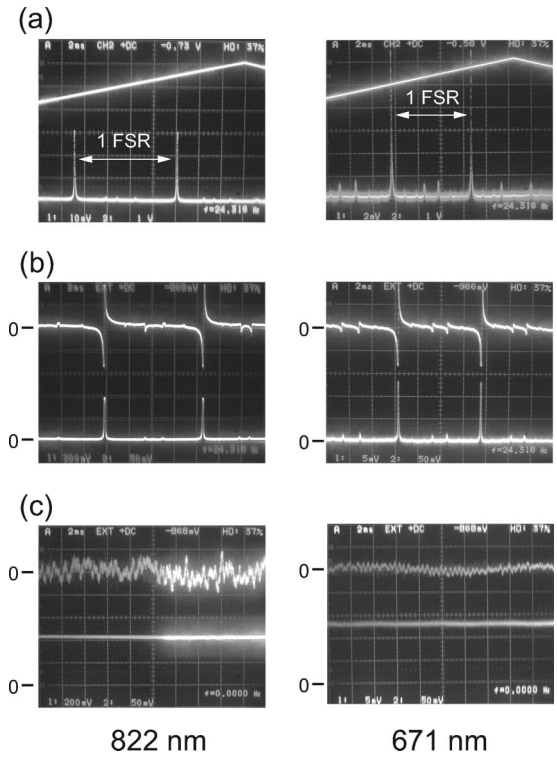

Fig. 2. Resonance signals and polarization spectroscopic signals of external cavity at 822 nm (left) and 671 nm (right). (a) Resonance signals by detection of the beams leaked through a concave mirror. Upper trace shows the voltage applied to the PZT for linearly scanning the cavity length. (b) Polarization spectroscopic signals (upper trace) and resonance signals (lower trace) when the cavity length was linearly scanned. (c) Same as (b) when servo loops were closed. All traces were obtained at the maximum fundamental powers, except (a) at 822 nm, where the power was decreased to avoid broadening of the resonance signal caused by the saturation of the photodiode. The traces in (b) and (c) are on the same scales.

ment factors A_i from the equation $A_i = (1 - R_i)/[1 - (R_i V_i)^{1/2}]^2$, where R_i are the input mirror reflectivities and the attenuation factors V_i are defined as $V_i = 1 - L_i$, where L_i are the fractions of the round-trip losses [19]. The attenuation factors V_i are estimated from the measured finesses F_i by using the relationship $F_i = \pi(R_i V_i)^{1/4}/[1 - (R_i V_i)^{1/2}]$. From the measured finesses and input mirror reflectivities, we estimate A_1 and A_2 to be 46 and 37, respectively. We conclude that the theoretically estimated sum-frequency power is $P_3 = (4.6 \times 10^{-1}\mathrm{W}^{-1})P_1P_2$, and we can generate a sum-frequency power of 2.4×10^{-4}W at the maximum available input powers. Considering the transmissivities at the crystal facet and of the concave mirror at 370 nm, the measured sum-frequency power was 58% of the theoretically estimated value. If the two beams are focused more tightly to realize the best focusing for $\xi = 1.39$ [13], we expect that the sum-frequency power would increase by approximately 40% owing to the increase in h.

Figure 4 shows the absorption spectrum of the $^2S_{1/2} - {}^2P_{1/2}$ transitions in Yb^+ ions in a hollow cathode lamp (Hamamatsu L2783) obtained by linearly sweeping the voltage applied to the PZT to control the cavity length. We found that the sum frequency was continuously frequency tunable over the range of 4 to 6 GHz.

With regard to the optical damage of the crystal, the sum-frequency power decreased by 10% of the initial value after operation for several hours. The rate of decrease was reduced when the power decreased below 50 μW. This damage appears to be permanent, and we need to change the position of the beams in the crystal when the sum-frequency power finally decreases below 30 μW, which is required to easily conduct laser cooling. It is unclear whether the damage is caused by UV radiation generated by the SFM.

B. Laser Cooling of Trapped Yb^+ Ions

We apply this light source to the laser cooling of $^{174}Yb^+$ trapped in an RF trap in order to confirm whether its performance is sufficient for laser cooling. The trap apparatus is similar to that used in our previous work [20] and is briefly described here. The minimum inner diameter of the ring electrode and the minimum distance between the endcap electrodes are 5 and 3.54 mm, respectively. The RF driving frequency and its typical amplitude are 2.2 MHz and 140 V, respectively. Two compensation electrodes are introduced to cancel stray DC fields that move the trapped ions from the trap center and enhance micromotion. We apply compensation voltages to one of the endcap electrodes and the two compensation electrodes to minimize the micromotion. The pressure of the chamber in which the trap electrodes are placed is 10^{-8} Pa. To load Yb^+ ions into the trap, we conduct photoionization of Yb atoms [21,22] of a natural isotope mixture from an oven. We adopt a scheme of two-step excitation of Yb atoms: We drive the $^1S_0 - {}^1P_1$ transition in Yb atoms at 399 nm as the first excitation, and the ions are produced by the second excitation from the $^1P_1$ state beyond the ionization potential. The lasers used for the first and the second excitations are a frequency-doubled Ti:sapphire laser [23] and an ECLD at 394 nm. To maintain the cooling cycle, depletion of the $^2D_{3/2}$ metastable state that is populated through the $^2P_{1/2}$ state with spontaneous emission is required. We drive the $^2D_{3/2} - {}^3D[3/2]_{1/2}$ transition at 935 nm [24] with radiation from an ECLD. The frequency of this repumping laser is stabilized to the resonance of a reference cavity, the spacer of which is made of Super Invar. The resonance frequency of the cavity is tuned by the rotation of an intracavity galvoplate.

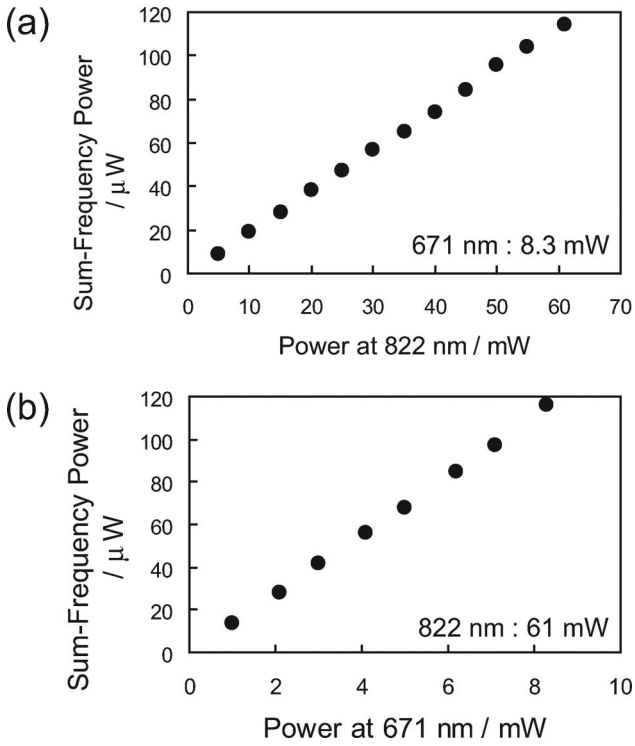

Fig. 3. Sum-frequency power versus fundamental powers at (a) 822 nm and (b) 671 nm, while the other fundamental power was fixed at the maximum available power indicated in the figures.

The sum-frequency beam is focused around the trap center using a lens with a focal length of 300 mm. The beam shape around the focus showed an astigmatism owing to the walk-off of the crystal used for the SFM. The beam sizes at the half-maximum intensity measured outside the trap were 55×450 μm and 200×170 μm at the focus of one axis and of the other one, respectively. These focuses were separated by approximately 25 mm along the beam. The other three beams are focused using a lens with a focal length of 1000 mm. The power of each laser beam at the window of the trap is approximately 50 μW, 3 mW, 100 μW, and 100 μW at 370, 935, 399, and 394 nm, respectively. The fluorescence from Yb^+ in the trap is collected by a lens and is detected using a photomultiplier tube, the output of which is measured by photon counting. To remove the fluorescence from Yb atoms, an interference bandpass filter at 370 nm is used.

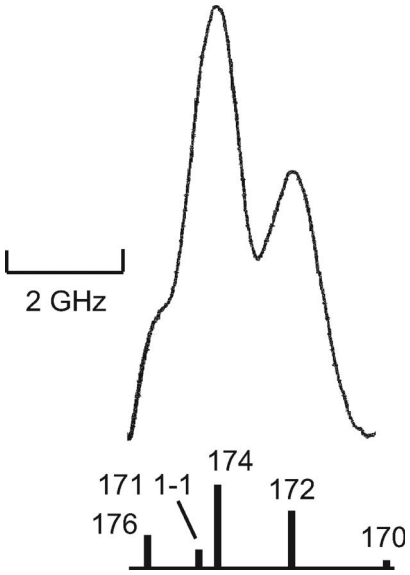

Fig. 4. Sample of linear absorption spectra of the $^2S_{1/2} - {}^2P_{1/2}$ transitions in Yb^+ in a hollow cathode lamp. Relative strengths and frequency separations of related isotopes are indicated.

To trap and laser-cool Yb^+ in the trap, we heat the oven and introduce the four laser beams simultaneously through the trap center. The frequency of the sum frequency, i.e., the cooling radiation, is adjusted to a few hundred megahertz lower than the center frequency of the cooling transition with reference to a linear absorption signal of Yb^+ in a hollow cathode lamp. The frequency of the repumping laser at 935 nm is roughly tuned using a wavemeter (Burleigh WA1500) with a resolution and uncertainty of 1×10^{-6}. After the fluorescence of Yb^+ is observed, the frequency is adjusted to maximize the fluorescence. The frequency of the first-excitation laser for photoionization is adjusted by the detection of a linear absorption signal in another hollow cathode lamp. Although the resonance of ^{174}Yb is not coincident with the peak of the linear absorption signal in the lamp owing to the overlap of the Doppler-broadened lines of the isotopes, the signal is a useful reference considering that the detuning from the absorption peak is resonant to the transition of ^{174}Yb.

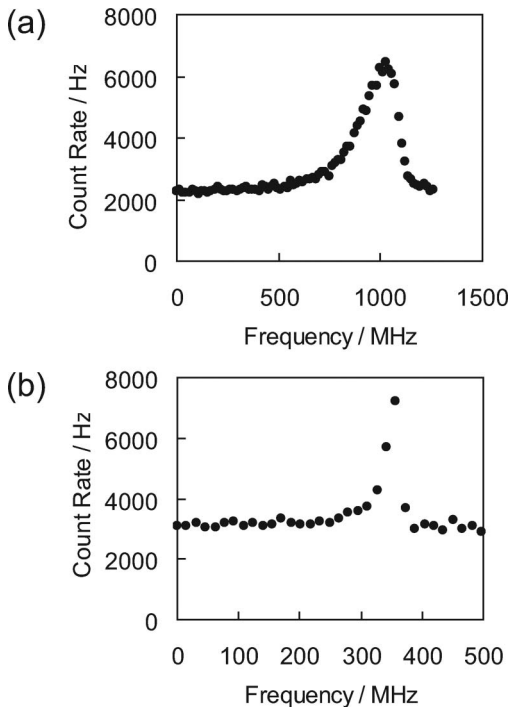

Fig. 5. Fluorescence spectra of the $^2S_{1/2} - {}^2P_{1/2}$ transitions in laser-cooled trapped $^{174}Yb^+$ obtained by the frequency sweep of the sum frequency: (a) large number of ions and (b) from 2 to 4 ions.

Figure 5(a) shows a sample of the spectra of a large number of laser-cooled trapped $^{174}Yb^+$ obtained by the frequency sweep of the cooling radiation generated by the SFM from low to high frequency. Figure 5(b) shows a sample of the spectra of a small number, from 2 to 4, of trapped $^{174}Yb^+$. To decrease the number of loaded ions, we decreased the current of the oven and shortened the duration of irradiation of the lasers used for ionization. After we loaded a small number of $^{174}Yb^+$, we adjusted the compensation voltages to narrow the spectra as we detect the spectra by the frequency sweep of the sum-frequency radiation. Figure 5(b) was obtained after the adjustment of the compensation voltages.

The result shown in Fig. 5(a) indicates that the sum-frequency radiation is suitable as cooling radiation to trap and cool Yb^+, and that shown in Fig. 5(b) indicates that the sum-frequency radiation has the potential for laser cooling single Yb^+ in the Lamb–Dicke region. The spectral width observed in Fig. 5(b) was twice as large as the natural linewidth of the cooling transition of 20 MHz. This was caused by saturation broadening and imperfections in the cancellation of the stray DC field.

4. Conclusions

We developed a continuous-wave tunable UV light source having a wavelength of 370 nm by the SFM of radiation from two ECLDs having wavelengths of 822 and 671 nm. Without using any optical amplifiers, we generated a sum-frequency power of more than 100 μW by using an external cavity that is simultaneously resonant at two fundamental wavelengths. Alignment and mode matching to the external cavity were achieved simultaneously for the two fundamental beams, locking of the two laser frequencies to the cavity resonances was stable, and the sum frequency was tunable over several gigahertz. Therefore, the SFM using a doubly resonant external cavity is a useful method for the generation of radiation at a wavelength that is difficult to obtain by second-harmonic generation. As a demonstration of the usefulness of this method, we successfully applied the sum-frequency radiation to the laser cooling of trapped Yb^+.

The early stage of this work was conducted at the National Research Laboratory of Metrology, which has been reorganized to be part of the Advanced Institute of Science and Technology, and we thank Akinori Wakita and Aoi Nakata for their assistance

with this part of our work. We also thank Yugo Onoda for the contributions to the photoionization studies, Yuya Miyoshi for the development of the SFM system, and Keita Mochizuki for the development of the ECLD. We are grateful to Yoichi Kawakami of Kyoto University and the Nichia Corporation for providing the UV diode laser.

References

1. T. Schneider, E. Peik, and C. Tamm, "Sub-hertz optical frequency comparisons between two trapped $^{171}Yb^{+}$ ions," Phys. Rev. Lett. **94**, 230801 (2005).
2. K. Hosaka, S. A. Webster, A. Stannard, B. R. Walton, H. S. Margolis, and P. Gill, "Frequency measurement of the $^{2}S_{1/2}$ – $^{2}F_{7/2}$ electric octupole transition in a single $^{171}Yb^{+}$ ion," Phys. Rev. A **79**, 033403 (2009).
3. S. Olmschenk, K. C. Younge, D. L. Moehring, D. N. Matsukevich, P. Maunz, and C. Monroe, "Manipulation and detection of a trapped Yb^{+} hyperfine qubit," Phys. Rev. A **76**, 052314 (2007).
4. C. Tamm, "A tunable light source in the 370 nm range based on an optically stabilized, frequency-doubled semiconductor laser," Appl. Phys. B **56**, 295–300 (1993)
5. K. B. MacAdam, A. Steinbach, and C. Wieman, "A narrow-band tunable diode laser system with grating feedback, and a saturated absorption spectrometer for Cs and Rb," Am. J. Phys. **60**, 1098–1111 (1992).
6. D. Kielpinski, M. Cetina, J. A. Cox, and F. X. Kärtner, "Laser cooling of trapped ytterbium ions with an ultraviolet diode laser," Opt. Lett. **31**, 757–759 (2006).
7. K. Sasaki, K. Sugiyama, V. Barychev, and A. Onae, "Two-photon spectroscopy of the 6S-8S transitions in cesium using an extended-cavity diode laser," Jpn. J. Appl. Phys. **39**, 5310–5311 (2000).
8. S. Olmschenk, D. Hayes, D. N. Matsukevich, P. Maunz, D. L. Moehring, K. C. Younge, and C. Monroe, "Measurement of the lifetime of the $6p\ ^{2}P^{\circ}_{1/2}$ level of Yb^{+}," Phys. Rev. A **80**, 022502 (2009).
9. D. J. Berkeland, F. C. Cruz, and J. C. Bergquist, "Sum-frequency generation of continuous-wave light at 194 nm," Appl. Opt. **36**, 4159–4162 (1997).
10. T. Fujii, H. Kumagai, K. Midorikawa, and M. Obara, "Development of a high-power deep-ultraviolet continuous-wave coherent light source for laser cooling of silicon atoms," Opt. Lett. **25**, 1457–1459 (2000).
11. K. Sugiyama, A. Wakita, and A. Nakata, "Diode-laser-based light sources for laser cooling of trapped Yb^{+} ions," in *Conference Digest of Conference on Precision Electromagnetic Measurements*, J. Hunter and L. Johnson, eds. (IEEE, 2000), pp. 509–510.
12. T. W. Hänsch and B. Couillaud, "Laser frequency stabilization by polarization spectroscopy of a reflecting reference cavity," Opt. Commun. **35**, 441–444 (1980).
13. G. D. Boyd and D. A. Kleinman, "Parametric interaction of focused Gaussian light beams," Appl. Phys. **39**, 3597–3639 (1968).
14. S. Guha and J. Falk, "The effects of focusing in the three-frequency parametric upconverter," J. Appl. Phys. **51**, 50–60 (1980).
15. H. Y. Shen, W. X. Lin, R. R. Zeng, Y. P. Zhou, G. F. Yu, C. H. Huang, Z. D. Zeng, and W. J. Zhang, "Twice sum-frequency mixing of a dual-wavelength Nd:$YALO_3$ laser to get 413.7 nm violet coherent radiation in $LiIO_3$ crystal," J. Appl. Phys. **70**, 1880–1881 (1991).
16. R. C. Eckardt, H. Masuda, Y.-X. Fan, and R. L. Byer, "Absolute and relative nonlinear optical coefficients of KDP, KD*P, BaB_2O_4, $LiIO_3$, MgO:$LiNbO_3$, and KTP measured by phase-matched second-harmonic generation," IEEE J. Quantum Electron. **26**, 922–933 (1990).
17. D. A. Roberts, "Simplified characterization of uniaxial and biaxial nonlinear optical crystals: a plea for standardization of nomenclature and conventions," IEEE J. Quantum Electron. **28**, 2057–2074 (1992).
18. R. C. Miller, "Optical second harmonic generation in piezoelectric crystals," Appl. Phys. Lett. **5**, 17–19 (1964).
19. M. Brieger, H. Büsener, A. Hese, F. V. Moers, and A. Renn, "Enhancement of single-frequency SHG in a passive ring resonator," Opt. Commun. **38**, 423–426 (1981).
20. K. Sugiyama, "Laser cooling of single $^{174}Yb^{+}$ ions stored in a RF trap," Jpn. J. Appl. Phys. **38**, 2141–2147 (1999).
21. K. Hosaka, S. A. Webster, P. J. Blythe, A. Stannard, D. Beaton, H. S. Margolis, S. N. Lea, and P. Gill, "An optical frequency standard based on the electric octupole transition in $^{171}Yb^{+}$," IEEE Trans. Instrum. Meas. **54**, 759–762 (2005).
22. C. Balzer, A. Braun, T. Hannemann, C. Paape, M. Ettler, W. Neuhauser, and C. Wunderlich, "Electrodynamically trapped Yb^{+} ions for quantum information processing," Phys. Rev. A **73**, 041407(R) (2006).
23. Y. Onoda, M. Ikeda, K. Sugiyama, H. Yokoyama, and M. Kitano, "Maximization of second-harmonic power using normal-cut nonlinear crystals in a high-enhancement external cavity," Appl. Opt. **48**, 1366–1370 (2009).
24. A. S. Bell, P. Gill, H. A. Klein, A. P. Levick, C. Tamm, and D. Schnier, "Laser cooling of trapped ytterbium ions using a four-level optical-excitation scheme," Phys. Rev. A **44**, R20–R23 (1991).